Circulation Control Airfoils as Applied to Rotary-Wing Aircraft

N. J. Wood*
Stanford University, Stanford, California
and
Jack N. Nielsen†
NASA Ames Research Center, Moffett Field, California

Nomenclature

c = airfoil chord
c_d = corrected section drag coefficient
c_{d_e} = effective drag coefficient
$c_{d_{\text{rake}}}$ = uncorrected drag coefficient from wake survey
c_ℓ = section lift coefficient
c_m = pitching moment about the half-chord
C_μ = blowing momentum coefficient, $= m \cdot V_j / (q_\infty \cdot S)$
h = slot height
m = jet mass flow
M_∞ = freestream Mach number
q_∞ = freestream dynamic pressure
s = chordwise slot location
S = wing reference area
V = velocity
α = angle of attack

Subscripts

j = jet parameter
∞ = freestream condition

I. Introduction

CIRCULATION control airfoils utilize a jet of air discharged along the upper surface of the airfoil near the trailing edge to increase and control the circulation and hence the airfoil lift. Such airfoils are of great interest for application to both fixed- and rotary-wing aircraft. For fixed-wing, their application to STOL aircraft has been shown[1-4] to reduce takeoff and landing speed, while their application to transport aircraft could permit larger payloads. Both applications take advantage of the high lift capability of the airfoils. For rotorcraft, the ability of circulation control airfoils to vary lift independent of incidence offers an opportunity to eliminate mechanical cyclic and collective pitch (to simplify the hub arrangement) and to incorporate higher harmonic blowing to reduce vibration.[5,6] New concepts such as the X-wing stopped rotor vehicle[7] offer the advantages of both hover capability in rotary-wing mode and high-speed cruise capability in the fixed-wing mode. The emphasis in this paper is on airfoils for rotor and stopped rotor application.

The purpose of this paper is to present an overview of the status of circulation control airfoils past and present and to suggest promising lines of inquiry for future research. It is hoped that the paper will stimulate innovative thinking and future research by bringing to the attention of a wider audience some of the challenges and potential payoffs associated with circulation control airfoils. The emphasis in the paper is directed toward an understanding or identification of some of the aerodynamic phenomena involved, together with some suggestions for future research activities.

II. Background and History

Early Work Abroad

The Coanda effect,[8] which underlies all circulation control airfoils, was inadvertently discovered by Henri Coanda,[9] a Romanian, in about 1910. He fitted metal plates to his airplane wings to deflect the exhaust and thus avoid burning the wooden wings. Instead of being deflected, however, the exhaust adhered to the plates and turned the flow over the curved surface. A summary of jet-flap and circulation control recently presented by Poisson-Quinton[10] includes information on research prior to 1960.

Norman J. Wood is a Research Assistant at the Joint Institute for Aeronautics and Acoustics. Dr. Wood was involved in the development of circulation control airfoils for application to the RSRA/X-wing vehicle with particular emphasis on the two- and three-dimensional performance characteristics. He is currently working in the area of direct flow control through the use of tangential and normal jet flows with applications to both fixed- and rotary-wing vehicles and performance at extreme angles of attack. Dr. Wood received his Ph.D from the University of Bath, England in 1981 and is a member of the AIAA.

Jack N. Nielsen is the Chief Scientist. Dr. Nielsen began his career in 1943 with the National Advisory Committee for Aeronautics (NACA). His extensive research during his 15 years with NACA provided the basis for his book *Missile Aerodynamics*, published in 1960. This book rapidly became the standard reference work in the field. In 1958, Dr. Nielsen helped form Vidya Corporation, where he served as Director of Research until 1965, when he left to found Nielsen Engineering & Research, Inc. (NEAR). At NEAR, he served as President. Dr. Nielsen received his M.S. in Mechanical Engineering and his Ph.D in Aeronautics from the California Institute of Technology. He is a member of the National Academy of Engineering and Fellow of AIAA.

Presented as AIAA Paper 85-0204 at the AIAA 23rd Aerospace Sciences Meeting, Reno, NV, Jan. 14-17, 1985; received April 24, 1986; revision received July 2, 1986.

A substantial effort to develop circulation control airfoils was begun by the National Gas Turbine Establishment[11] in England in about 1960. At the same time similar work was conducted by Lockwood.[12] The paper of Cheeseman[11] describes the work of the National Gas Turbine Establishment up to 1967. Section characteristics of circulation control airfoils with blowing were measured. One result of interest is that hysteresis was observed when the jet detached from the model and the lift fell abruptly. In addition, a circulation control rotor was built and tested to obtain typical performance figures. A system of higher harmonic cyclic control of the blades also using hub throttling is described. Two possible arrangements of VTOL circulation control stopped rotor transports were proposed. The designs are of interest in that two-bladed rotors, stopped in the streamwise direction, were involved. In one case, each wing is equipped with a rotor. These designs suggest the possibility of utilizing a two-bladed stopped rotor in an oblique-wing application.

Theories for circulation control airfoils of circular form were developed in Great Britain during and following this period. These will be reviewed under the theoretical section.

An interesting piece of experimental work on a cylindrical circulation control airfoil was published by Lockwood[12] in 1960. The circular cylinder had from one to eight blowing slots and achieved very high lift coefficients: 19 with two slots, 18 with one slot, much of which was at very high blowing momentum and thus included a fair amount of vertical thrust component. The angular orientation of the slot was the principal parameter affecting the maximum lift coefficient. One point of interest is that the work was motivated by a desire to reduce the landing speed of hypersonic aircraft.

Mention should also be made of the experimental work of Kind,[13] Jones,[14] and Wood,[15] each of whom attempted to measure the turbulence properties in the highly curved wall jet on a circulation control airfoil.

Work in the United States

The principal efforts in the United States on circulation control airfoils have been carried out by the David Taylor Model Basin (DTMB), later renamed the David Taylor Naval Ship Research and Development Center (DTNSRDC). This effort started with experimental results for an elliptical cambered airfoil, published in 1970.[16] In the next few years, a large amount of work on circulation control airfoils and rotors was accomplished at DTNSRDC. A listing of the published reports, together with abstracts, is given in Englar.[17]

The work at DTNSRDC has been to extend the development of circulation control airfoils and to assemble a data base. Some of the parameters investigated are airfoil section thickness and camber, slot height and position, blowing rate, angle of attack, Mach number, and shape of Coanda surface. A particularly significant effort was carried out to develop efficient transonic circulation control airfoils.

Recently, in addition to DTNSRDC, NASA Ames has performed extensive tests on a series of circulation control airfoils. To supplement the performance data, a number of flow visualization studies have been performed, including holographic interferometry and shadowgraph of the trailing-edge flowfield.[18]

Harvell and Franke[19] present recent data on a cambered elliptical airfoil section taken at the Air Force Institute of Technology and reference earlier work. Some unsteady aerodynamic results for a circulation control airfoil are presented by Schmidt.[20]

Tabulated data for a number of airfoils have been furnished to the authors through the courtesy of the personnel at DTNSRDC. A description of these airfoils and the range of their test parameters are listed in Table 1. For each airfoil listed, the thickness and camber distributions are given, together with data on the radius and type of the Coanda surface and the position of the slot on the airfoil, where available. The ranges of the test parameters are given.

The reference list provided does not cover the entire range of experiments that have been performed; however, it does represent some of the more acceptable work from considerations such as model design and consistency of data.[21-30] In many cases, a detailed analysis of the individual data set is included within the reference.

III. Typical Data for Circulation Control Airfoils

It is of interest to illustrate the general aerodynamic behavior of a circulation control airfoil and to see how it differs from that of a conventional airfoil. When applied to stopped rotor vehicles, the airfoils are required to be fore-and-aft symmetric to satisfy the conditions for trimmed stopped rotor flight. In some instances, the data presented here does not completely meet this requirement and, in many cases, only trailing-edge blowing slots were included in the wind tunnel models for simplicity of construction.

Lift Characteristics

The most fundamental characteristic of circulation control airfoils is their ability to produce extremely high lift coefficients at low speed, and this has been amply demonstrated in many of the early reports.[1,5,16] Lift coefficients of 6 or 7 are typical. Indeed, sectional lift coefficients approaching the theoretical inviscid maximum of $2\pi(1+t/c)$ have been demonstrated. This was a primary reason for the application of the circulation control concept to rotary-wing aircraft. The capability to produce high lift on the retreating blade at high advance ratios suggests the possibility for trimmed operation at high forward speed. Unfortunately, the high lift coefficients achieved at low speed also complicate the estimation of the

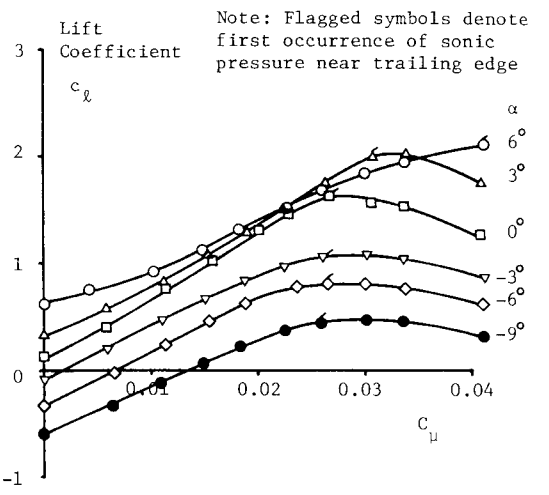

Fig. 1 Lift characteristics of airfoil 103*XW* at $M_\infty = 0.4$.

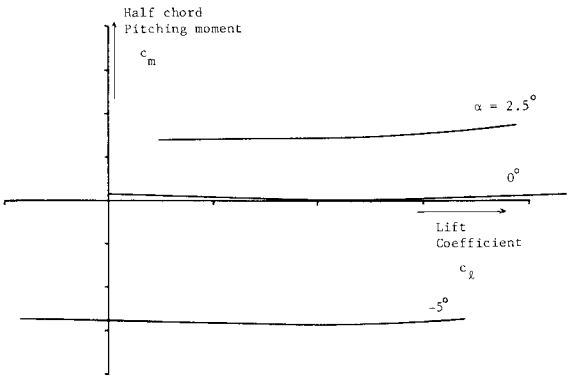

Fig. 2 Moment coefficient about the half-chord vs blowing momentum.

Table 1 Test airfoil parameters

Airfoil designation	t/c, %	Camber, %	s/c	r/c	Chord, in.	Mach range	Alpha range	Ref.
20/0	20	0	0.97	0.039	7.908	0.12	−20, +8	21
15RND	15	0	0.96	0.040	7.700	0.3,0.9	−1.2	22
15PURE	15	0	0.924	0.0112	8.000	0.3,0.9	−1.2	22
NCCR1513-7559E	15	1.3	0.975	0.020	8.000	0.12	−20, +6	23
NCCR1510-7067N	15	1	0.967	[a]	8.000	0.12	−20, +6	24
NCCR1510-7567S	15	1	0.974	[a]	8.000	0.12	−20, +10	24
NCCR1505-7567S	15	0.5	0.97	[a]	7.991	0.12	−20, +10	25
NCCR1610-8054S	16	1[b]	0.98	[a]	8.000	0.12	−12, +6	26
103*XW*	16	1[b]	0.969	0.028	18.00	0.3,0.8	−12, +6	27
103*DE*	16	1[b]	0.964	0.017	18.00	0.3,0.8	−9, +6	27

[a]Information not published. [b]Asymmetric (noncircular).

degree of tunnel interference on the results obtained from two-dimensional testing. Thus, in the interest of clarity, recent wind tunnel results obtained over a wider speed range will be used to demonstrate the key features of the concept.

Figure 1 shows the variation of airfoil lift coefficient with C_μ for various values of angle of attack for airfoil 103*XW*[27] at $M_\infty = 0.4$. It is generally noted that c_ℓ peaks at some intermediate value of C_μ and produces the C_μ stall defined as the condition at which lift augmentation ratio is zero. As reported, the pressure corresponding to sonic flow, C_p^*, is usually reached on the Coanda surface slightly before the stall, as indicated by the flagged symbols.

Most of the data for negative angles of attack exhibit linear curves of c_ℓ vs C_μ, as well as linear curves of c_ℓ vs α. Most applications of circulation control airfoils for rotorcraft are confined to the negative angle-of-attack range for reasons that are explained by Wilkerson.[31]

The lift augmentation ratio $\partial c_\ell / \partial C_\mu$ is the rate of response of the lift coefficient due to change in the blowing momentum coefficient. A value of 10 indicates that the jet is 10 times more efficient in the production of lift by circulation control than it would be on an inertial basis with the jet vertical.

It should be noted that the essentially linear behavior demonstrated is applicable to the low to moderate C_μ ranges. At higher blowing levels, which are common at low speeds, a general square-root dependency of c_ℓ on the blowing parameter is exhibited.

Moment Characteristics

It is interesting to note that under the usual definition of aerodynamic center (the point about which there is constant pitching moment), no such point exists on a circulation control airfoil. If one considers the case of constant angle of attack, an aerodynamic center due to blowing can be shown to exist just aft of the midchord. If however, constant blowing is assumed, a second aerodynamic center near the quarter-chord is apparent. In either case, a change in one controlling parameter produces a change in the constant pitching moment about the other aerodynamic center, invalidating the general definition.

Figure 2 shows the moment coefficient about the midchord for a typical circulation control airfoil, the data having been corrected to free air conditions by the matching of the experimental distributions with those produced from an inviscid calculation at a similar lift coefficient. Until the recent work of Wood and Rogers,[32] it was assumed that there were two contributions to midchord moment, incidence and blowing, indicated by the decreasing values of C_m with increasing blowing strength that were usually illustrated. That research, however, has subsequently shown that the midchord moment is decoupled from the blowing rate and hence the lift coefficient due to blowing. All the previous data exhibit a coupled trend due to the lift interference of the wind tunnel boundaries. This observation may be used to observe the effects of lift interference on previous data and also to correct lift coefficients to free air conditions. This result also has significant impact on the torsional design of rotor blades.

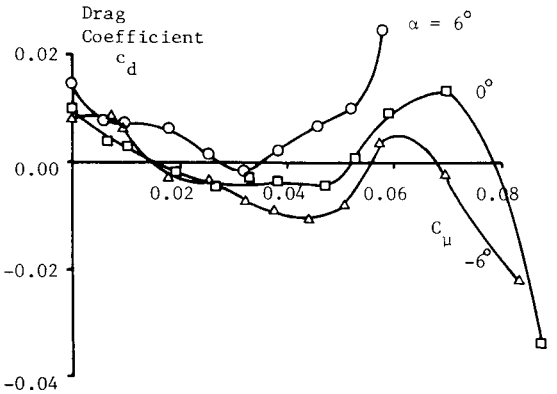

Fig. 3 Drag coefficient vs blowing momentum coefficient for airfoil 103*XW* at $M_\infty = 0.3$.

Drag and Lift/Drag Ratio Characteristics

The drag coefficient is frequently measured by a rake behind the airfoil, using the methods of Betz and Jones.[33] Since neither method accounts for the additional momentum introduced by the jet, the wake drag coefficient is often corrected as follows[34]:

$$c_d = c_{d_{\text{rake}}} - (mV_\infty/qc) = c_{d_{\text{rake}}} - C_\mu (V_\infty/V_j) \qquad (1)$$

Values of c_d are plotted vs C_μ in Fig. 3 for three angles of attack at $M_\infty = 0.3$ for airfoil 103*XW*.[27] It is noted that the drag coefficient can be negative if the net effect of the jet is propulsive. Except for certain isolated flow cases such as shock-dominated flowfields, the drag is not predictable at the present state of the art, and the trends of the data in Fig. 3 are difficult to explain satisfactorily. It could, however, be considered that the effect of the jet is to remove the momentum deficit at least from the upper surface boundary layer, with an accompanying reduction in drag. The general trends are the same for all three angles of attack except at the higher values of the blowing parameter.

Clearly the measured values of c_d shown in Fig. 3 require additional correction terms to develop a lift-drag ratio parameter that can be compared to that for conventional airfoils. Some account should be taken of the power necessary to produce the kinetic energy of the jet. If we assume a perfect nozzle so that power required is the kinetic energy of the jet per unit time, then an incremental drag coefficient associated with the kinetic energy of the jet is[22]

$$\Delta c_d = \frac{1}{V_\infty} \frac{\text{d(KE)}}{\text{d}t} = \frac{1}{V_\infty} \frac{mV_j}{2qc} = C_\mu \frac{V_j}{2V_\infty} \qquad (2)$$

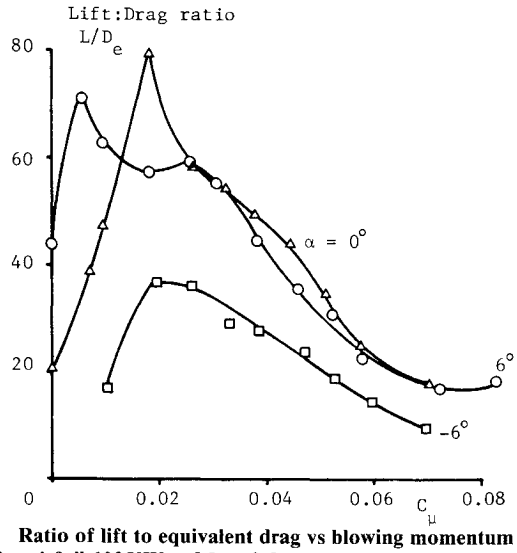

Fig. 4 Ratio of lift to equivalent drag vs blowing momentum coefficient for airfoil 103*XW* at $M_\infty = 0.3$.

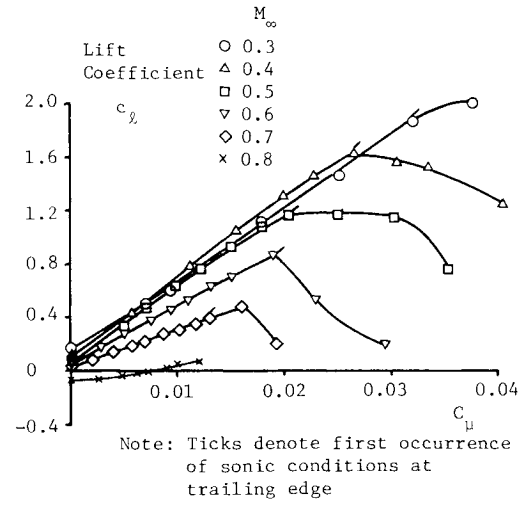

Fig. 5 Lift coefficient vs blowing momentum coefficient for airfoil 103*XW* at $\alpha = 0$ deg.

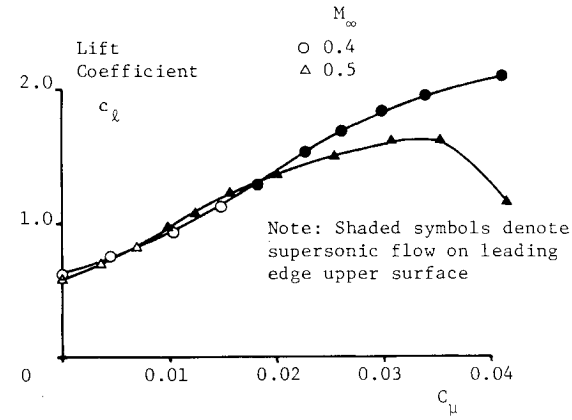

Fig. 6 Operation in the presence of supersonic flow regions for airfoil 103*XW* at $\alpha = 6$ deg.

With this correction, the equivalent drag coefficient is

$$c_{d_e} = c_d + C_\mu (V_j/2V_\infty) \tag{3}$$

Another correction is sometimes added to account for intake momentum flux in the form of $C_\mu \cdot V_\infty/V_j$. In this paper, we will use Eq. (3). The above procedure permits comparison of drag results for conventional airfoils with those for blown airfoils.[30] However, a more relevant method for making such comparisons has yet to be established.

The ratios of lift to equivalent drag based on Eq. (3) are given in Fig. 4 for the 103*XW* airfoil at $M_\infty = 0.3$. It is noted that substantial values of the ratio are obtained at the lower blowing rates. For high values of C_μ, the corrective term in Eq. (3) can be an order of magnitude greater than c_d. The low lift-drag ratio at high C_μ (and hence high c_l) is thus associated with the compressor power to generate the jet kinetic energy. Since circulation control airfoils are primarily high lift devices, the lower values of lift-drag ratio may be of little consequence with respect to the absolute values of the lift that may be generated.

IV. Some Parametric Dependencies of Circulation Control Airfoils

Introductory Remarks

In the previous section, some of the more basic characteristics of circulation control airfoils were described: high lift, low drag, and pitching moments due to angle of attack only. We will now attempt to clarify some of the more important effects, including nonlinearities, due to the other parameters, for example slot height, slot position, Mach number, and angle of attack. Only a small number of references with sufficient information are available to enable a study of these characteristics to be performed. Englar[22] first described the effects of Mach number on a 15% ellipse for three different trailing-edge geometries. One was a jet flap and thus will not be considered except to note that it exhibited a lift augmentation ratio approximately one order of magnitude less than the two circulation control configurations. The other two geometries were a pure ellipse and a rounded trailing edge, each having a different slot location. Wilkerson and Montana[26] and Abramson and Rogers[27] conducted experiments on a 16%-thick section with a variety of trailing-edge configurations, including a circular arc, a log spiral, and a displaced ellipse. Unlike those of Englar,[22] the slot location was similar for all three configurations, providing some valuable information on the effects of trailing-edge geometry. All three tests covered a Mach number range of up to at least $M_\infty = 0.8$ for a range of angles of attack from -9 to $+6$ deg. Wood and Conlon[28] considered the performance of a 20%-thick elliptical airfoil with 3% camber over a similar speed range but only for a single slot height and a single circular-arc-type trailing-edge configuration. More recently an extensive sequence of experiments have been performed at NASA Ames Research Center on a variety of elliptic airfoils (designed by DTNSRDC), which had similar slot locations and trailing-edge designs. These experiments have provided significant information to clarify many of the aerodynamic phenomena encountered in the previous wind tunnel tests.

Before a detailed discussion of the aerodynamics, it is necessary to comprehend the basic fluid mechanics of circulation control; two concepts are important. First, it is the velocity difference between the jet and the local stream that produces the entrainment of the upper boundary layer into the jet. Second, it is suggested that the ratio of the jet momentum to the boundary-layer momentum deficit determines the lift increment due to blowing. One would expect that conditions that thicken the boundary layer approaching the slot (and hence increase the momentum thickness) would tend to reduce the effectiveness of the jet for a given jet momentum and velocity difference and that conditions that tend to increase the velocity difference at the slot for a given momentum ratio would tend to improve the mixing rate between the two streams, leading to higher lift augmentations. The following sections will show evidence to confirm these simple physical concepts. The initial discussion will concentrate on the effects

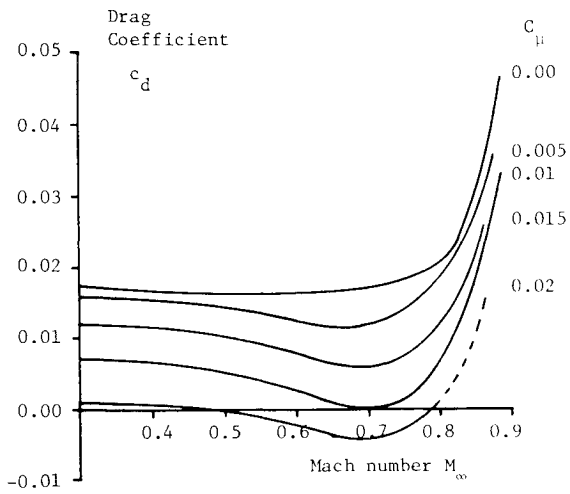

Fig. 7 Drag variation with Mach number for pure-ellipse trailing edge, from Ref. 22.

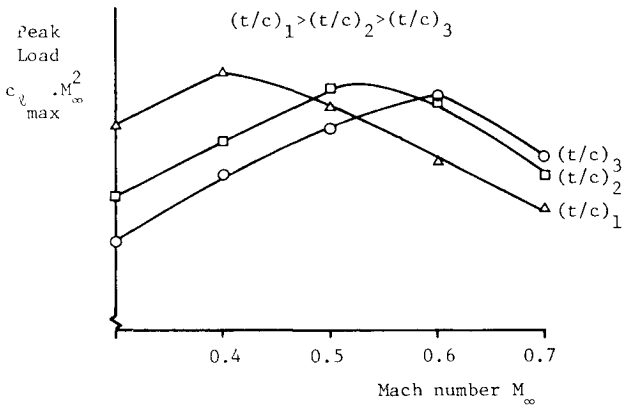

Fig. 8 Peak load as a function of Mach number for different thickness-ratio airfoils.

of Mach number, angle of attack, Coanda geometry, and slot height. A further section will then consider the stall phenomena that have been identified, C_μ stall and angle-of-attack stall.

Parametric Discussion

Effects of Mach Number

Figure 5 shows the effects of increasing Mach number on the lift production of the 103*XW* airfoil.[27] Two effects are apparent: first, the maximum lift coefficient due to blowing that can be produced before a stall occurs decreases significantly as the Mach number increases. Second, the lift augmentation ratio is reduced at Mach numbers above 0.5 for the airfoil presently under consideration. The thickness of the boundary layer approaching the slot is a function of the angle of attack, the circulation, and the Mach number. If only the Mach number is increased, then the boundary-layer thickness increases due to the accentuated pressure gradients imposed around the airfoil. Thus, for a given jet momentum, one would expect a reduced augmentation, as is the case. In the limit, if a shock occurs on the upper surface, then the sudden resultant increase in the boundary-layer thickness downstream should further reduce the lift augmentation. An example of this is given in Fig. 6, where the change in lift augmentation, once the shock is of sufficient strength to affect the boundary layer, is visible.

Drag rise, one of the usual effects of Mach number, is also present on circulation control airfoils. By the time this situation occurs, the effect of the jet momentum is so reduced that blowing has little effect on the point at which drag rise appears, as can be seen in Fig. 7, from Englar.[22]

It is of interest to note that an airfoil of given thickness and camber ratio will exhibit a peak load at a Mach number dependent on that thickness and camber ratio. As one might expect, the thinner, less cambered sections peak at the higher Mach numbers. Figure 8 illustrates the effect for a number of airfoils, and the actual peak load can be seen to be almost invariant with airfoil thickness (t/c), an interesting result considering the high lift coefficients achieved at low Mach numbers.

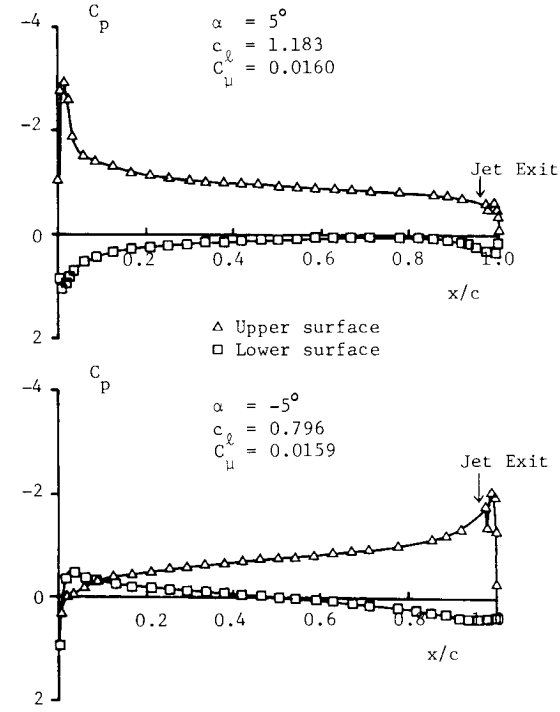

Fig. 9 Effect of angle of attack on the pressure distribution around a circulation control airfoil at $M_\infty = 0.4$ for constant blowing momentum.

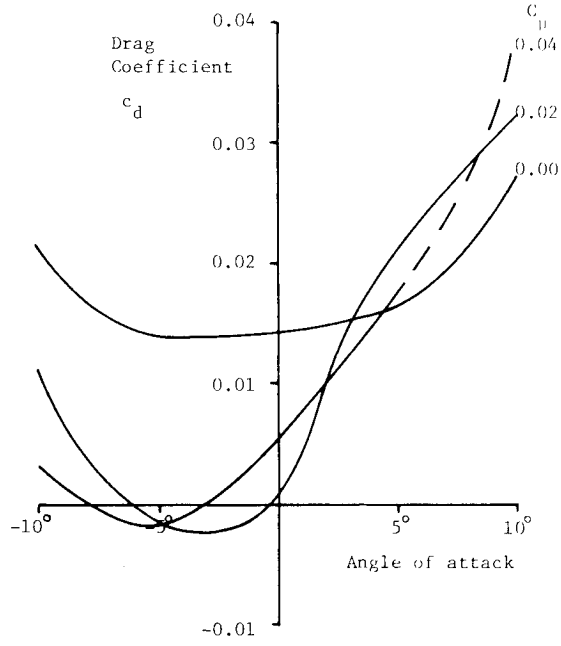

Fig. 10 Effect of angle of attack on drag coefficient for a typical circulation control airfoil at $M_\infty = 0.4$.

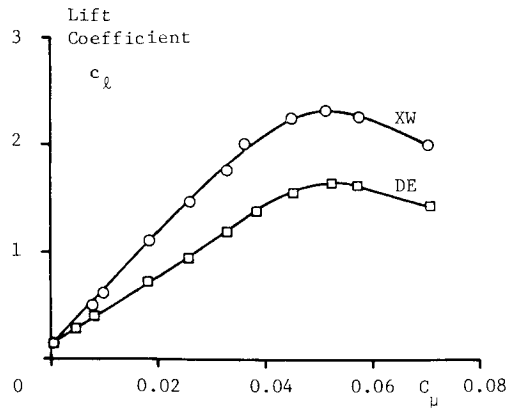

Fig. 11 Effect of trailing-edge geometry on lift generation at $M_\infty = 0.3$.

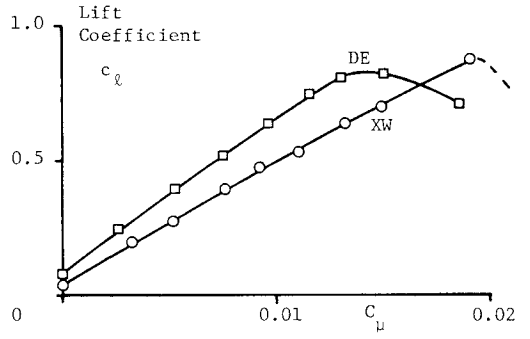

Fig. 12 Effect of trailing-edge geometry on lift geometry at $M_\infty = 0.6$.

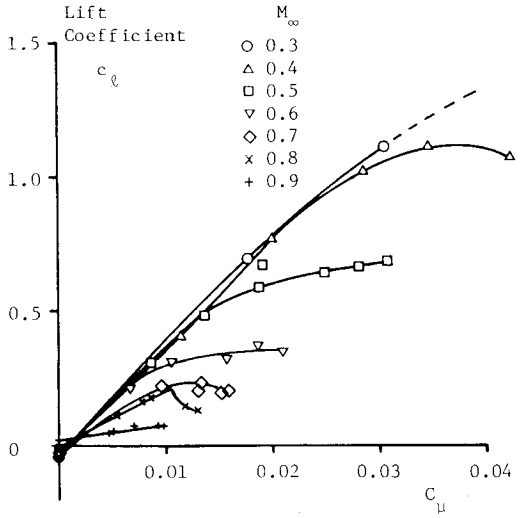

Fig. 13 Effect of Mach number on lift generation for rounded ellipse.

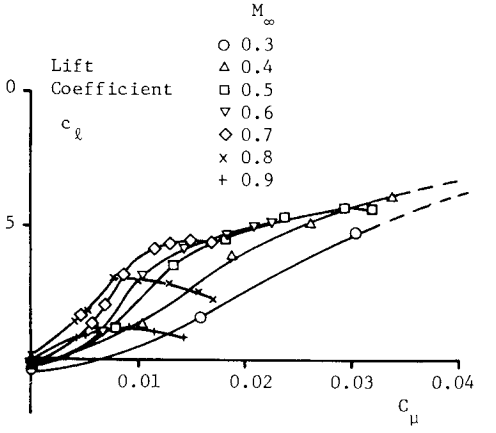

Fig. 14 Effect of Mach number on lift generation for pure ellipse.

Effects of Angle of Attack

The leading-edge condition that produces an angle-of-attack or "alpha" stall on conventional airfoils, namely, the adverse pressure gradient at the leading edge, impacts the performance of circulation airfoils. However, the effect on performance is noticeable at angles of attack far below the usual stall boundaries. Consider the two pressure distributions shown in Fig. 9. For the positive angle of attack, the upper surface boundary layer is growing in a much more severe pressure gradient, producing a higher value of momentum thickness at the slot exit. One would therefore expect that for the same jet momentum, the higher angle of attack would produce less lift due to blowing since the momentum ratio is reduced. Figure 1 confirms the expected trends and emphasizes the nonlinearity of the performance at positive angles of attack. To complement the reduction of lift augmentation, the airfoils also exhibit an increased wake drag (as opposed to effective drag) at positive angles of attack compared to negative (see Fig. 10). Note that the reduced lift augmentation occurs before there is any evidence of alpha stall, at angles of attack between 0 and +5 deg, a result dependent on the thickness, camber, and leading-edge geometry of the airfoil.

Effect of Coanda Geometry

The results of Abramson and Rogers[27] are perhaps the only reliably consistent data to evaluate the performance of different Coanda geometries over a range of Mach numbers. Figures 11 and 12 summarize the findings for two of the three different trailing edges. In all three cases, the slot position was held nominally constant (compared to Englar[22]). Details of the geometries are given in the reference and in Table 1. Examination of the results for $M_\infty = 0.3$, Fig. 11, shows that the circular arc (*XW*) exhibits improved lift augmentation capabilities compared to the displaced ellipse (*DE*). Figure 12 shows the performance of the same two airfoils at a Mach number of 0.6; it is interesting to note the reversal of the trends. At the present time, the reasons for these characteristics are not clear; however, it appears there are two primary phenomena to be considered. First, the local radius of curvature of the Coanda surface is important in determining the degree of instability of the jet layer. Second, a certain rate of momentum transfer is necessary between the jet and the upper surface boundary layer to maintain the turning of the flow around the Coanda surface. The experimental data would appear to suggest that the distribution of curvature around the Coanda surface could be optimized for a given set of operating conditions; however, a satisfactory scheme is not yet available.

Englar[22] reports data on a 15% thick, uncambered, elliptic section for three different trailing-edge configurations over a range of Mach numbers at an angle of attack of −1.2 deg. Excluding the jet-flap configuration that is reported, consider the differences between the rounded trailing edge and the pure-ellipse trailing edge. Both were tested at similar slot heights, but the actual slot locations were quite different. For the rounded trailing edge, the slot was at 96% chord and the trailing-edge radius was 4.0% chord, while the pure-ellipse slot was at 92.4% chord and the trailing-edge radius was 1.1% chord. The lift performance of the two airfoils is compared in Figs. 13 and 14. At low speeds the rounded-trailing-edge airfoil produces substantially higher lift augmentations than the pure ellipse. At high speeds, however, the situation is reversed, illustrating the same phenomenon that was present between the 103 *DE* and the 103*XW*. It is possible that the more forward slot location and reduced slot exit curvature may be

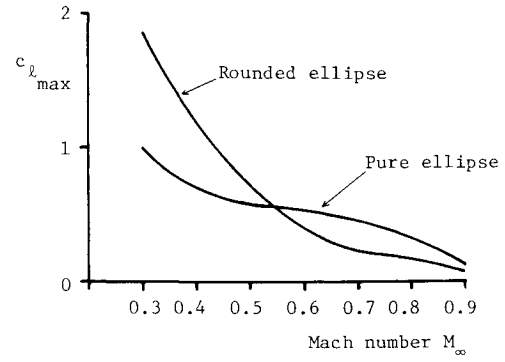

Fig. 15 Maximum lift coefficient as a function of Mach number for the rounded and pure ellipses.

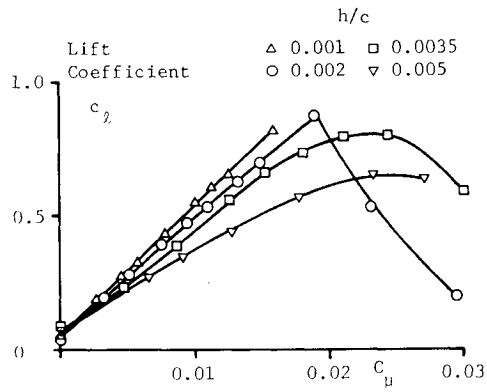

Fig. 16 Effect of slot height on lift generation as a function of blowing momentum coefficient for airfoil 103*XW* at $M_\infty = 0.6$.

more efficient at high speeds due to the increased aerodynamic time for mixing to occur. Figure 15 shows the reversal in airfoil performance in terms of the peak lift coefficient attained as a function of Mach number at a fixed geometric incidence of -1.2 deg. Unfortunately, the experiments are not sufficiently controlled to enable positive conclusions to be drawn, and it should be remembered that both the slot position and the Coanda surface curvature distribution were varied.

Effect of Slot Height

The effect of varying the slot height of a circulation control airfoil provides an interesting illustration of the compromise between the advantages of high jet velocity or high jet momentum. Figure 16 shows the lift generated at a fixed Mach number and zero angle of attack for a range of slot heights as a function of C_μ, the jet momentum coefficient. Interestingly, smaller slot heights exhibit higher lift augmentation ratios, presumably as a result of their higher jet velocity for a given C_μ. The higher velocities promote more rapid mixing between the jet and the boundary layer.

Stall Conditions

Two distinct types of stall have been identified for circulation control airfoils. They are the C_μ stall, where the lift augmentation ratio is zero, and the angle of attack stall (or alpha stall), where the lift curve slope is zero. The C_μ stall may be further subdivided into a jet (C_p^*) stall and a jet detachment stall. Each of these will be addressed independently in the following sections.

Jet (C_p^* Stall)

This is perhaps the most commonly observed stall over a range of Mach numbers 0.2–0.7. The C_p^* stall is identified by the maximum lift condition which coincides approximately with the first occurrence of the pressure corresponding to

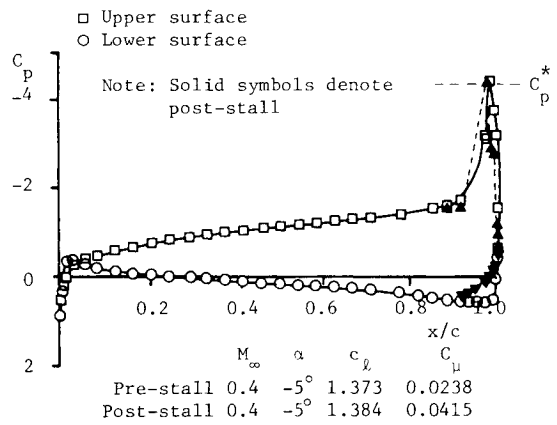

Fig. 17 Pre- and post-C_μ stall pressure distributions for a typical circulation control airfoil.

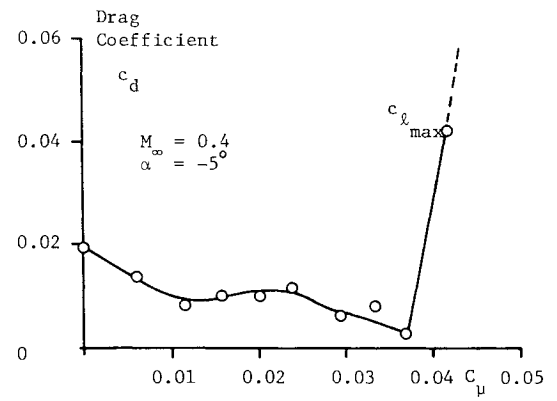

Fig. 18 Effect of C_μ stall on drag coefficient for a typical circulation control airfoil.

sonic flow anywhere on the trailing-edge Coanda surface. Figure 1 showed an example of the lift production vs C_μ, and on each curve the first point matching the sonic criterion was indicated. Since the criterion is relatively simple and potential flow tends to model the pressure distributions tolerably well,[27] these simple tools can be used to evaluate the maximum lift due to blowing for a variety of airfoils. Figure 17 shows examples of the actual pressure distributions recorded on a circulation control airfoil, pre- and post-stall, at approximately the same lift conditions. One can observe that no separation is evident at any point on the airfoil surface; indeed, the suction around the trailing edge usually increases just after stall, and the loss in lift is associated with a general loss of suction over the entire upper surface. For the particular case illustrated, conditions of similar lift coefficient pre- and post-stall have been considered to show the similarity of the pressure distributions and their dependence primarily on the lift coefficient. It is postulated that the stall mechanism is associated with a sudden breakdown of the mixing process at some point downstream of the slot exit. The reduction in mixing should produce an increase in the measured drag coefficient as confirmed in Fig. 18. It has also been observed that the wake flow becomes very unsteady post-stall as evidenced by measured wake profiles. The occurrence of sonic pressure conditions downstream of the slot does not appear to be linked with the appearance of choked jet conditions. However, a strong slot height and Coanda geometry dependence has been noted. At smaller slot heights, a considerably higher jet pressure ratio is required to achieve a jet stall condition although the increment in lift due to blowing at stall may be similar. Also, for highly curved Coanda surfaces, the appearance of the sonic condition occurs at somewhat lower jet pressure ratios since the acceleration of the fluid is greater.

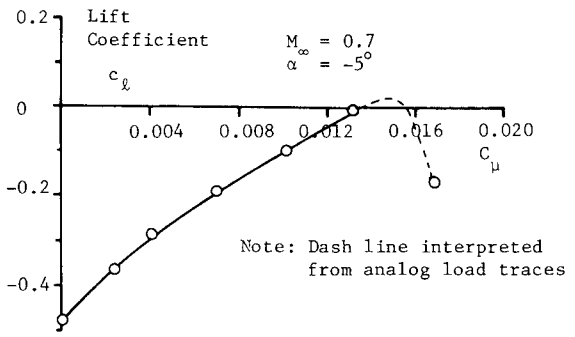

Fig. 19 A typical jet detachment stall.

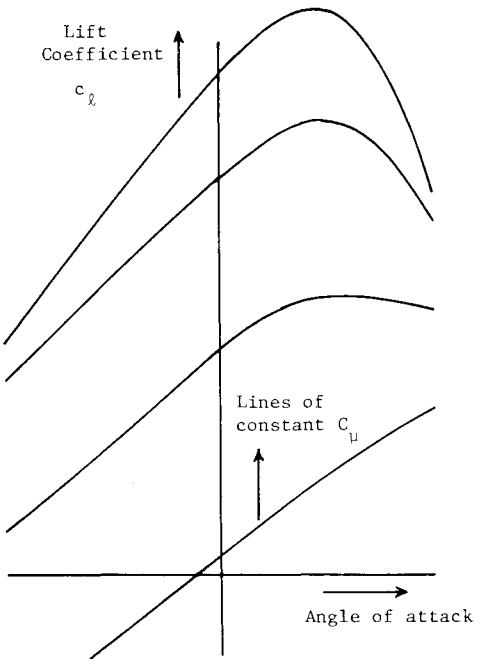

Fig. 20 Lift production for constant blowing conditions for a typical circulation control airfoil at $M_\infty = 0.4$.

Jet Detachment

The jet detachment stall is evidenced by a total loss of suction around the trailing edge, producing a sharp drop in lift compared to the smooth curve usually associated with jet stall. The jet detaches from the Coanda surface a short distance from the slot exit and the mixing between the jet and the upper surface boundary layer is greatly reduced. From examination of a range of data, the jet detachment stall occurs primarily in regions where high momentum deficits exist in the upper surface boundary layer. Thus, one would expect jet detachment to occur at high Mach numbers and high angles of attack. Also, where high pressure ratios are required to achieve a given lift increment (i.e., small slot heights or low lift augmentation ratio), a jet detachment stall may occur before a jet stall limit is reached, especially for small r/c. Figure 19 illustrates a typical lift curve where a jet detachment stall has occurred although the lack of data points does not truly depict the severity of the lift dropoff. An analog load technique described in Ref. 27 was used to provide more information regarding the actual stall point.

Angle-of-Attack Stall

As previously discussed, the lift curve slope becomes nonlinear at positive angles of attack due to the increasingly adverse pressure gradients at the leading edge of the airfoil. In the limit, it is possible to produce a leading-edge separation

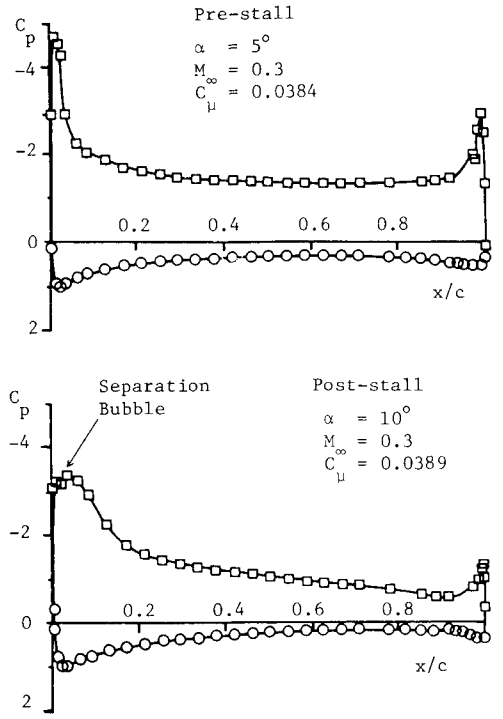

Fig. 21 Pre- and post-alpha stall pressure distributions for a typical circulation control airfoil.

followed by a turbulent reattachment while still maintaining some degree of lift augmentation. To illustrate this angle-of-attack stall (or alpha stall), it is necessary to examine the performance of a circulation control airfoil in terms of its lift curve slopes. By plotting the lift coefficient against the angle of attack for constant blowing momentum, the occurrence of alpha stall is clearly defined (Fig. 20). The phenomenon is a function of leading-edge geometry and circulation since the separation may occur at angles well below the usual unblown stall points. As the circulation is increased by the introduction of jet momentum at the trailing edge, so the leading-edge stagnation point moves around the leading edge toward the lower surface, producing higher fluid accelerations. Thus, an alpha stall may occur at an angle of attack at which the unblown flow was attached. Clearly, simple examination of the performance with respect to C_μ is insufficient for full evaluation since the lift augmentation may remain positive (but reduced) even in the presence of an alpha stall. Figure 21 illustrates the pressure distributions for an airfoil in the presence of alpha stall. Note the small separation region at the leading edge and the quick reattachment. The effect of the alpha stall is to cause a rapid thickening of the upper surface boundary layer, which will cause a reduction in the lift augmentation for a given blowing momentum.

The alpha stall is particularly relevant to thinner circulation control airfoils due to the higher accelerations experienced at the leading edge. The problem is familiar to designers of advanced rotorcraft airfoil sections. The solution for circulation control sections is more complex, however, since the leading edge must also function as a trailing edge over part of the rotor disk.

V. Theory of Circulation Control Airfoils

The theory of circulation control airfoils has been gradually developed over a period of years. The first efforts were for the most part carried out in Great Britain. More recently, powerful Computational Fluid Dynamics computer methods have been brought to bear on the problem, but a completely satisfactory design code is still not available.

Early Theory of Circular Airfoils and Coanda Surfaces

Newman[35] considered the two-dimensional case of a circular airfoil with a tangential jet in still air. He succeeded in correlating the surface pressure distributions, the position of separation, and related quantities based on dimensional analysis and simplifying assumptions. Newman concluded that the entrainment by the jet of the surrounding fluid is an essential physical feature of the flow. He further deduced that the normal pressure stress $\overline{v'^2}$ is significant compared to the pressure drop across the flow. The method of Dunham[36] may represent the earliest method for predicting lift of circulation control airfoils with external flow and several slots.

The work of Kind[37] is related to that of Dunham and represents a considerable extension. The configuration used for the analysis was an elliptical cross-section wing with a blowing slot on the upper surface close to the 96% chord location and a Coanda surface with a uniform radius of almost 4% of the chord. The objective was to determine C_μ for a given c_ℓ, or vice versa. Kind showed that measured velocity profiles on a Coanda surface could be well fitted by a formulation due to Spalding, except in the inner layer near separation. Increased entrainment due to wall curvature was estimated using experimental data taken in still air on a cylinder with a blowing slot. To determine c_ℓ, C_μ was iterated until the separation pressures on the upper and lower surfaces were equal (the Thwaites criterion). The method gave excellent agreement with measured overall jet thicknesses and the decay in peak velocity in the wall jet. However, the value of C_μ to develop a given c_ℓ was not predicted very well, and the error increased with the angle of attack.

A computer method for calculating the incompressible case has been developed by Dvorak[38] and Dvorak and Kind.[39] It has been exercised in an optimization procedure by Tai, Kidwell, and Vanderplatts.[40] We now describe the incompressible method of Dvorak.[38] The first step is to compute the airfoil pressure distribution for a given lift coefficient, using potential theory based on a vortex lattice arrangement utilizing panels with linearly varying distribution of vorticity with continuity at panel edges. Once the pressure distribution is established, the boundary layer flow on the lower surface is calculated using integral methods that account for the laminar, transition, and turbulent regions. The calculations are continued to the separation point on the lower surface. The boundary layer development on the upper surface is then calculated to the slot, using integral methods. From the slot to the upper surface separation point, a finite difference technique is used, and the radial pressure gradients are accounted for in the static pressure. A modified Van Driest eddy viscosity model is used in the inner region, but the outer region utilizes a different eddy viscosity model due to Dvorak,[41] which is meant to account for the effects of curvature.

Once the viscous calculations have been made, the effect of the boundary layer on the potential flow is represented by a distribution of sources, the strengths of which are determined by the boundary-layer displacement thickness. The potential flow is again calculated and the iterative process repeated to convergence. The above procedure is incorporated in the computer code CIRCON.

TRACON, a computer program for calculating the flow around circulation control airfoils at transonic speed is described by Dvorak and Choi.[42] The general iterative procedure described previously with respect to CIRCON is retained for the transonic case. However, the vortex lattice program has been replaced with a full-potential code. By this change, the problem of locating the rear stagnation point at the juncture of vortex panels is avoided.

The boundary-layer calculation procedures are changed to account for compressibility, and the part of the boundary layer downstream of the blowing slot is solved by a finite difference scheme similar to that of CIRCON. The eddy-viscosity model is the same as for CIRCON.

Comparison between prediction and experiment generally shows good overall agreement for pressure distribution for both low and transonic speeds at negative angles of attack, but the pressures are not well predicted over the upper surface near the trailing edge. The authors suggest that this is possibly due to the fairing in of the slot required by the analysis, which results in slightly different contours between experiment and analysis.

Additional efforts have been made to improve the TRACON program, and the work to date, although not complete, is described in Ref. 43. The first problem addressed is the lack of sensitivity to small Coanda surface modifications due to the semiempirical approach to computing additional suction pressures induced by the jet. The second problem is the inability to resolve the flow downstream of choked nozzles because of the lack of underexpanded jet capability. The approach being used is to couple a new wall jet calculation procedure with TRACON. The new wall jet procedure, called SPLITJET, is due to Dash and Beddini[44] and Dash et al.[45] The joining of the two codes is not complete.

More recently, Shrewsbury[46] has used the compressible Reynolds time-averaged Navier-Stokes equations to solve the flowfield around a two-dimensional circulation control airfoil. The scheme utilizes a body-fitted coordinate system with a modified algebraic turbulence model to define the turbulence characteristics of the flow. Reasonable agreement with experiment is obtained, with the exception of the prediction of the shear layers within the wall jet as the flow approaches separation. For this reason, the code is thought to lack general applicability until such time as an improved turbulence modeling scheme becomes available.

Pulliam et al.[47] have also considered this problem. A novel mapping of the flowfield was developed, based on a spiral grid emanating from the jet slot. The spiral then continuously wraps around the airfoil to the far field. This produces an extremely fine grid spacing through the wall jet region, with no compromise on run time. Solution of the thin layer approximation of the Navier-Stokes equations with an algebraic turbulence model with no curvature corrections produced some favorable results. However, inclusion of an arbitrary constant curvature correction to the shear stress produced extreme sensitivity of the lift coefficient to the value of the constant for any given, fixed Coanda surface.

VI. Future Research Areas for Circulation Control Airfoils

The aerodynamics of circulation control airfoils, while well advanced both experimentally and theoretically, still needs further development for practical application to flight vehicles. By presenting brief descriptions of some of the challenges ahead, it is our hope that some researchers may be encouraged to study them.

Turbulence Modeling

The specification of a turbulence model for a Coanda flow is hampered by the lack of data for validating the various available models. Some velocity profiles and static-pressure measurements are available for subsonic curved wall jets, but none appear available for supersonic jet flow. The case for an external stream also appears to be somewhat limited. It is of great importance to measure accurately the turbulent stresses in the wall jet flowfield, including the normal and shear stresses. The recent work of Novak[48] has suggested that progress in measurement techniques may soon yield a standard set of results that should include controlled variations in slot height to Coanda radius. Consideration should be given to the extremely high turbulence levels expected, the small scale of the flow, and the high turbulent fluctuation frequencies that will be present in the flow. This remains the key factor in the success of any numerical modeling of the two-dimensional circulation control flowfield.

Drag

It is of interest to compare the drag and lift-drag ratio of a circulation control airfoil with those for conventional airfoils. However, the drag measurements of circulation control airfoils must be adjusted for several factors before the comparison can be made. The drag wake surveys must be corrected for the momentum of the air issuing, in a bounded tunnel test section, from the airfoil slot. Further adjustments are made for the power expended by the compressor in producing the kinetic energy of the jet and for the inlet momentum flux. Several possible systems for adjusting the drag are described by Englar,[22] one a force-based coefficient and one an energy-based coefficient. Assumptions concerning inlet loss, compressor efficiencies, etc., are made in the treatment. It is suggested that a standard method for expressing drag be developed so that all data on circulation control airfoils be directly comparable.

Unsteady Aerodynamics

In many applications, circulation control airfoils experience rapid variations in angle of attack, Mach number, and blowing level. Their use in rotors (other than in the hover mode) exemplifies such an application. The conversion maneuver to stopped rotor flight and blade flutter are other cases of unsteady flow. The amount of data on unsteady aerodynamics of circulation control rotors is sparse and needs to be greatly expanded. At the same time, codes to calculate the unsteady aerodynamics of the airfoils are nonexistent.

Supersonic Airfoils

An interesting question is whether circulation control airfoils have application to supersonic speed operation. For a two-dimensional airfoil with an attached shock, the Kutta condition is not operational at supersonic speeds. For detached shocks the situation is not clear. For supersonic flow over the upper rear surface of the airfoil, the jet would have to be underexpanded to transfer momentum to the boundary layer.

Aerodynamic Efficiencies

The suitability of a circulation control airfoil for certain applications may also depend on its lift-drag ratio, in addition to its total lifting capability and controllability. Attempts have been made to increase the efficiencies of circulation control airfoils at transonic speeds by raising their critical Mach numbers. However, optimization of the airfoil parameters for lift-drag ratio has not been attempted. This task is ideal for a future computer code that could predict accurately the characteristics of circulation control airfoils. At this time the codes do not yield reliable drag estimates. Further work on the techniques, both subsonic and transonic, will in time correct this deficiency, and the important question of aerodynamic efficiency may be resolved.

Three-Dimensional Aerodynamics

Recently, Wood[49] reported an experiment on a three-dimensional circulation control wing with and without wing sweep. The results indicated that conventional sweep theory is equally applicable to circulation control and that little or no secondary effects on the entrainment were evident. The finite root and tip introduced strong secondary vortices shed into the wake from the ends of the blowing jet and presumably would impact the downwash distribution along the span. Additional experimentation is required to further evaluate the forward swept case and to examine the effects of spanwise nonuniformity of slot height, slot position, or airfoil section.

VII. Concluding Remarks

Circulation control has potential for a number of significant advances in aeronautics. First, it has the capability to produce high lift coefficients without the necessity of going to high angles of attack. Second, it has the potential to minimize rotor vibration by the use of higher harmonic control. Third, it eliminates the presence of hinges in helicopter applications.

At the present state of the art, researchers are trying to understand the aerodynamic phenomena underlying circulation control, and much progress has been made. While much progress has also been made in design codes for predicting the performance of circulation control airfoils and rotors, we are not yet in a position to design accurately for specific applications. However, this capability is under rapid development. The importance of developing this capability lies in the fact that numerous potential applications for circulation control could be evaluated, once accurate design means are available.

Acknowledgments

The authors gratefully acknowledge the cooperation and recommendations of the staff of the David Taylor Naval Ship Research and Development Center (DTNSRDC) in the preparation of this paper. In particular, we thank Mr. E.O. Rogers for his particular contribution not only to this paper but also to the technology in general.

References

[1]Englar, R.J. and Huson, G.G., "Development of Advanced Circulation Control Wing High Lift Airfoils," AIAA Paper 83-1847, July 1983.

[2]Englar R.J., "Development of the A-6/Circulation Control Wing Flight Demonstrator Configuration," DTNSRDC Rept. ASED-79/01, Jan. 1979.

[3]Loth, J.L. and Boasson, M., "Circulation Control STOL Wing Optimization," AIAA Paper 83-0082, Jan. 1983.

[4]Eppel, J.C., Shovlin, M.D., Jaynes, D.M., Englar, R.J., and Nichols, J.H., "Static Investigation of the Circulation Control Wing/Upper Surface Blowing Concept Applied to the Quiet Short-Haul Research Aircraft," NASA TM 84232, July 1982.

[5]Cheeseman, I.C. and Seed, A.R., "The Application of Circulation Control by Blowing to Helicopter Rotors," *Journal of the Royal Aeronautical Society*, Vol. 71, No. 848, July 1966, pp. 451–467.

[6]Rogers, E.O., "Recent Progress in Performance Prediction of High Advance Ratio Circulation Control Rotors," Paper 29, presented at the Sixth European Rotorcraft and Powered Lift Aircraft Forum, Bristol, England, Sept. 1980.

[7]Williams, R.M., Leitner, R.T., and Rogers, E.O., "X-wing: A New Concept in Rotary Wing VTOL," presented at the American Helicopter Society Symposium on Rotor Technology, Aug. 1976.

[8]Wilson, D., "An Experimental Investigation of the Mean Velocity, Temperature and Turbulence Fields in Plane and Curved Two Dimensional Wall Jets: Coanda Effect," Ph.D. Thesis, University of Minnesota, Minneapolis, 1970.

[9]Kirkpatrick, D.G. and Barnes, D.R., "Development and Evolution of the Circulation Control Rotor," Preprint 80-13, presented at the 36th Annual Forum of the American Helicopter Society, Washington, DC, May 1980.

[10]Poisson-Quinton, P., "The Jet Flap Story: An Opportunity for Wing/Propulsion Integration," 22nd Lanchester Memorial Lecture to the Royal Aeronautical Society, London, June 1982.

[11]Cheeseman, I.C., "Circulation Control and Its Application to Stopped Rotor Aircraft," Paper presented at the 10th Anglo-American Aeronautical Conference, Los Angeles, CA, Oct. 1967.

[12]Lockwood, V.E., "Lift on a Circular Cylinder by Tangential Blowing from Surface Slots," NASA TND-244, May 1960.

[13]Kind, R.J., "A Proposed Method of Circulation Control," Ph.D. Thesis, Cambridge University, England, 1967.

[14]Jones, D.G., "The Performance of Circulation Controlled Airfoils," Ph.D. Thesis, Cambridge University, England, 1970.

[15]Wood, N.J., "The Aerodynamics of Circulation Controlled Airfoils," Ph.D. Thesis, Bath University, England, 1981.

[16]Williams, R.M. and Howe, R.J., "Two-dimensional Subsonic Wind Tunnel Tests on a 20 Percent Thick, 5 Percent Cambered Circulation Control Airfoil," DTNSRDC Tech. Note AL-176, AD 877-764, Aug. 1970.

[17]Englar, R.J. and Applegate, C.A., "Circulation Control—An Updated Bibliography of DTNSRDC Research and Selected Outside References," DTNSRDC Rept. 84-052, Sept. 1984.

[18]Bachalo, W.D., "An Experimental Investigation of Circulation Control Flow Fields Using Holographic Interferometry," NASA CR 166482, Oct. 1982.

[19]Harvell, J.K. and Franke, M.E., "Aerodynamic Characteristics of a Circulation Control Elliptical Airfoil with Blown Jets," AIAA Paper 83-1794, July 1983.

[20]Schmidt, L.V., "Unsteady Aerodynamics of a Circulation Controlled Airfoil," Paper 12, presented at Fourth European Rotorcraft and Powered Lift Aircraft Forum, Stresa, Italy, Sept. 1978.

[21]Abramson, J., "Two Dimensional Subsonic Wind Tunnel Evaluation of a 20 Percent Thick Circulation Control Airfoil," DTNSRDC Rept. ASED 311, June 1975.

[22]Englar, R.J., "Two Dimensional Transonic Wind Tunnel Test of Three 15 Percent Thick Circulation Control Airfoils," DTNSRDC Rept. ASED 182, Dec. 1970.

[23]Abramson, J., "The Low Speed Characteristics of a 15 Percent Quasi Elliptical Circulation Control Airfoil with Distributed Camber," DTNSRDC ASED 79/07, May 1979.

[24]Abramson, J., "Two Dimensional Subsonic Wind Tunnel Evaluation of Two Related Cambered 15 Percent Thick Circulation Control Airfoils," DTNSRDC ASED 373, Sept. 1977.

[25]Abramson, J., "Low Speed Characteristics of a Circulation Control Airfoil Having Aft Camber and a Spiral Trailing Edge," DTNSRDC ASED 84/07, 1984.

[26] Wilkerson, J.B. and Montana, P.S., "Transonic Wind Tunnel Test of a 16 Percent Thick Circulation Control Airfoil with 1 Percent Asymmetric Camber," DTNSRDC ASED 82/03, April 1982.

[27]Abramson, J. and Rogers, E.O., "High Speed Characteristics of Circulation Control Airfoils," AIAA Paper 83-0265, Jan. 1983.

[28]Wood, N.J. and Conlon, J.C., "The Performance of a Circulation Control Airfoil at Transonic Speeds," AIAA Paper 83-0083, Jan. 1983.

[29]Ottensoser, J., "Two Dimensional Subsonic Evaluation of a 15 Percent Thick Circulation Control Airfoil with Slots at Leading and Trailing Edges," DTNSRDC Rept. 4456, July 1974.

[30]Englar, R.J., "Two Dimensional Subsonic Wind Tunnel Investigations of a Cambered 30 Percent Thick Circulation Control Airfoil," DTNSRDC Technical Note AL-201, May 1972.

[31]Wilkerson, J.B., "An Assessment of Circulation Control Airfoil Development," DTNSRDC Rept. 77-0084, Aug. 1977.

[32]Wood N.J. and Rogers E.O., "An Estimation of the Wall Interference on a Two-dimensional Circulation Control Airfoil," AIAA Paper 86-0738, March 1986.

[33]Schlichting, H., *Boundary Layer Theory*, 4th ed., McGraw-Hill, New York, 1960, pp. 616–620.

[34]Englar, R.J., "Subsonic Two-dimensional Wind Tunnel Investigation of the High Lift Capability of Circulation Control Wing Sections," DTNSRDC Rept. ASED-274, April 1975.

[35]Newman, B.G., "The Deflection of Plane Jets by Adjacent Boundaries—Coanda Effect," *Boundary Layer and Flow Control*, Vol. 1, edited by C.V. Lachman, Pergamon Press, Oxford, England, 1961, pp. 232–264.

[36]Dunham, J., "A Theory of Circulation Control by Slot Blowing Applied to a Circular Cylinder," *Journal of Fluid Mechanics*, Vol. 33, Pt. 3, 1968, pp. 495–514.

[37]Kind, R.J., "A Calculation Method of Circulation Control by Tangential Blowing Around a Bluff Trailing Edge," *Aeronautical Quarterly*, Vol. XIX, Aug. 1968, pp. 205–223.

[38]Dvorak, F.A., "A Viscous Potential Flow Interaction Analysis for Circulation Controlled Airfoils," Analytical Methods Inc., Redmond, WA, Rept. 75-01, Jan. 1975.

[39]Dvorak, F.A. and Kind, R.J., "Analysis Method for Viscous Flow over Circulation Controlled Airfoils," *Journal of Aircraft*, Vol. 16, Jan. 1979.

[40]Tai, T.C., Kidwell, G.H., and Vanderplatts, G.W., "Numerical Optimization of Circulation Control Airfoils," AIAA Paper 81-0016, Jan. 1981.

[41]Dvorak, F.A., "Calculation of Turbulent Boundary Layers and Wall Jets over Curved Surfaces," *AIAA Journal*, Vol. 11, April 1973, pp. 517–524.

[42]Dvorak, F.A. and Choi, D.A., "The Analysis of Circulation Controlled Airfoils in Transonic Flows," AIAA Paper 81-1270, June 1981.

[43]"Improved Algorithms for Analysis of Circulation Control Rotors," Analytical Methods, Inc., Redmond, WA, Rept. 8407, May 1984.

[44]Dash, S.W. and Beddini, R.A., "Viscous/Inviscid Analysis of Curved Wall Jets: Pt. 2, Viscous Pressure—Split Model (SPLITJET)," Science Applications, Princeton, NJ, TR-7, Nov. 1982.

[45]Dash, S.W., Beddini, R.A., Wolf, D.E., and Sinha, N., "Viscous/Inviscid Analysis of Curved Sub- or Supersonic Wall Jets," AIAA Paper 83-1679, July 1983.

[46]Shrewsbury G. "Numerical Evaluation of Circulation Control Airfoil Performance using Navier-Stokes Methods," AIAA Paper 86-0286, Jan. 1986.

[47]Pulliam, T.H., Jesperson, D.C., and Barth, T.J., "Navier-Stokes Computations for Circulation Control Airfoils," AIAA Paper 85-1587, July 1985.

[48]Novak, C.J. and Cornelius, K.C., "An LDV Investigation of a Circulation Control Airfoil Flowfield," AIAA Paper 86-0503, Jan. 1986.

[49]Wood, N.J., "The Section Characteristics of a Finite, Swept Circulation Control Airfoil," AIAA Paper 86-1817, June 1986.